DOI: 10.1002/masy.201300105

Structural Investigations of Titanium Metaphosphate Glasses by Ambient and High-Temperature X-Ray Diffraction Techniques

Nilay J. Lakhkar,[1] *Jonathan C. Knowles**[1,2]

Summary: This paper presents the structural characterization of melt-quenched titanium metaphosphate glasses having compositions of $0.5P_2O_5$–$0.4CaO$–$(0.1–x)Na_2O$–$xTiO_2$ ($x = 0.00$–0.07 mol fraction) by means of x-ray diffraction (XRD) techniques employed under both ambient and high-temperature conditions. Ambient XRD spectra of powdered glass samples revealed the amorphous nature of the glasses, while ambient XRD software analysis of crystallised glass powders provided information regarding the phase transitions in the glass compositions with an increase in the TiO_2 content. High-temperature XRD (HT-XRD) contour plots showed good agreement with the results of both ambient XRD and differential thermal analysis, thereby demonstrating the correspondence between three distinct sets of experimental data and allowing us to correlate thermal events with the crystalline phases formed. Thus, the overall results offer interesting clues into the structure of these titanium metaphosphate glasses, which have emerged as major candidates in the biomedical field for use as substrates in the regeneration of hard and soft tissues.

Keywords: differential thermal analysis; glass structure; x-ray diffraction; phosphate glasses; titanium

Introduction

Titanium phosphate glasses, and phosphate glasses in general, have attracted considerable interest in recent years for biomedical applications involving bone tissue regeneration.[1–5] The reasons for the suitability of these glasses are two-fold: on the one hand, the chemistry of these glasses allows for the glass degradation rate to be precisely controlled through changes in the glass composition, and on the other hand, these glasses have been demonstrated to provide a stable surface for the migration, attachment and proliferation of bone cells, with the ions released from the glasses being considered to play a significant role in eliciting a favourable response under both *in vitro* and *in vivo* conditions.[1,6–12] P_2O_5–Na_2O–CaO–TiO_2 titanium phosphate glasses are essentially inorganic polymer systems where P_2O_5 serves as the network former, Na_2O and CaO function as modifying oxides and TiO_2 is an intermediate oxide; in fact, it is possible for pure P_2O_5 glasses to be prepared, but the highly hygroscopic nature of P_2O_5 precludes the use of these glasses in applications, and thus the remaining oxides are added to reduce the glass dissolution rate.[5]

From a materials science perspective, titanium phosphate glasses are of interest because the glass structure is closely interlinked to its properties; for instance, wide variations in dissolution rates can be achieved by subtle variations in glass

---

[1] Division of Biomaterials and Tissue Engineering, Eastman Dental Institute, University College London, 256 Gray's Inn Road, London WC1X 8LD, UK
[2] Department of Nanobiomedical Science and WCU Research Center, Dankook University, Cheonan 330-714, Republic of Korea
E-mail: j.knowles@ucl.ac.uk

chemistry, either by changing the composition of the constituent oxides or by incorporating additional metal oxides such as ZnO or SrO.[7,8,13–15] To some extent, ongoing research in these glass systems is being driven by developments in the available characterisation techniques, which allows us to obtain information at various size scales from the macroscopic level down to the atomic level. Thus, glass bulk properties such glass density and surface free energy can be investigated using relatively simple techniques and equipment and at the same time information about the local environments and connectivities of constituent atoms such as P and Ti can be obtained by highly specialised techniques such as ^{31}P magic angle spinning nuclear magnetic resonance (^{31}P MAS-NMR) and Ti k-edge X-ray near edge structure (XANES).[16] In this study, we focus on one such technique, namely X-ray diffraction (XRD), to study the glass structure at the phase level. XRD experiments have been carried out under both ambient and high-temperature conditions, and the data from these experiments have been compared with information from differential thermal analysis (DTA) in order to investigate the correlations between these different techniques.

Materials and Methods

Glass Manufacture

Glasses with compositions listed in Table 1 were prepared according to previously described methods.[7,16] The following precursors (all with purities of >98% and obtained from VWR-BDH, Poole, UK) were used without further purification: phosphorus pentoxide (P_2O_5), calcium carbonate ($CaCO_3$), sodium dihydrogen orthophosphate (NaH_2PO_4) and titanium oxide (TiO_2). A total of 5 compositions were prepared (Table 1). Stoichiometric amounts of precursors were weighed and then mixed in a Seward Stomacher®400 Circulator (Wolf Laboratories, York, UK) at 200 rpm for 1 min. Because P_2O_5 is highly hygroscopic, care was taken to weigh the P_2O_5 precursor separately and add it quickly to the already mixed $CaCO_3$, NaH_2PO_4 and TiO_2 precursors, followed by further mixing for 1 min. The precursor mix was then poured into a Pt/10% Rh type 71040 crucible (Johnson Matthey, Royston, UK) and the crucible was placed in a Carbolite RHF 1500 furnace (Carbolite, Sheffield, UK) preheated at 700°C. The precursors were first heated at 700°C for 30 min to remove H_2O and CO_2 and then melted at the temperatures and times listed in Table 1. After melting for the required period, the glasses were rapidly quenched by pouring on to a steel plate at room temperature and then allowed to cool overnight. Glass powders for the below experiments were obtained by crushing glass fragments using a Retsch MM301 milling machine (Retsch, Germany).

Differential Thermal Analysis

DTA studies were performed on glass powders using a Setaram Differential Thermal Analyser (Setaram, France). Approximately 60 mg of glass powder was placed in a 10-μl platinum crucible

Table 1.
Glass compositions and codes used.

Glass code	Glass composition (mol%)				Melting temperature/time (°C/h)
	P_2O_5	CaO	Na_2O	TiO_2	
Ti0	50	40	10	–	1100/1
Ti1	50	40	9	1	1300/3
Ti3	50	40	7	3	1300/3
Ti5	50	40	5	5	1300/3
Ti7	50	40	3	7	1400/5

which was then placed in the analyser. DTA experiments were carried out by heating the sample from room temperature to 1000°C at a heating rate of $20°C.min^{-1}$ using air as the purge gas; an empty platinum crucible was used as a reference.

Ambient X-Ray Diffraction

Ambient XRD studies on the glasses were performed using powder forms of both the original glass samples and crystallised glass samples. For the crystallised samples, crystallisation of the glass was carried out by heating the glass powder in a Lenton furnace (Lenton, Hope Valley, UK) at a ramp heating rate of $7°C.min^{-1}$ to approximately 8–10°C above the crystallization temperature obtained from DTA, followed by crystallisation at the same temperature for 3 h; overnight cooling to ambient temperature at the same rate; and crushing of the crystallised glass samples to powder. The XRD analysis was carried out using a Brüker D8 Advance Diffractometer (Brüker, Coventry, UK) in flat plane geometry with Ni-filtered Cu $K\alpha$ radiation and a LynxEye detector (Brüker, Coventry, UK). Data was collected from $2\theta = 10°$ to 100° at a step size and count time of 0.02° and 0.1 s, respectively. For phase identification, the Crystallographica Search-Match software (Oxford Cryosystems, Oxford, UK) was utilized.

High-Temperature X-Ray Diffraction

The same Brüker D8 Advance Diffractometer as that used for normal XRD studies was used for high temperature XRD (HT-XRD) studies as well. In addition to the above mentioned LynxEye detector, an Anton Paar HTK 1600 heated stage (Anton Paar, Austria) fitted with a Pt electrode was used for the HT-XRD experiments. The HT-XRD data were collected at 2θ values in the range 20–40° for a step size and counting time of 0.02° and 0.1 s per point, respectively. As in the normal XRD experiments, the radiation used was Ni-filtered Cu $K\alpha$ radiation at a voltage of 35 kV and current of 45 mA. The temperature range applied for data collection was 30–1100°C at a heating rate of $21°C.min^{-1}$, and helium was used as the purge gas.

Results and Discussion

Ambient X-Ray Diffraction

The XRD patterns for the original glass samples are shown in Figure 1. All the XRD patterns were free from any detectable crystalline phases and broad peaks were observed at 2θ values of around 20–40°. This result was as expected and it indicated that all the prepared glasses were amorphous in nature, thereby demonstrating the success of the glass preparation process.

The X-ray diffraction patterns of the crystallised glass samples revealed that as the TiO_2 content of the glasses increased, the intensities of groups of peaks related to specific phases underwent changes as indicated by the dotted lines 1–5 in Figure 2. Analysis using Crystallographica software showed that the Ti0 and Ti1 glasses comprised sodium calcium phosphate [$NaCa(PO_3)_3$; ICDD no.: 23–669] as the main phase with calcium phosphate [CaP_2O_6; ICDD no.: 11–39] as the secondary phase. However, at higher TiO_2 contents, the main phase experienced a transition from $NaCa(PO_3)_3$ to CaP_2O_6. This is to be expected because the Na_2O content of the glasses decreases from 10 mol % to 3 mol% as TiO_2 is incorporated into the glass at the expense of Na_2O while the P_2O_5 and CaO contents remain constant. At a TiO_2 content of 3 mol%, the main and secondary phases were CaP_2O_6 and $NaCa(PO_3)_3$, respectively. However, at TiO_2 contents of 5 mol% and higher, a metallic titanium phosphate [TiP_2O_7; ICDD no.: 34–1468] phase was observed as the secondary phase.

The transition between the phases as evidenced by software analysis helps to explain the variation in the intensities of certain peaks. For example, the peaks denoted by dotted lines 1 and 2 in Figure 2 occur at 2θ values values of approximately

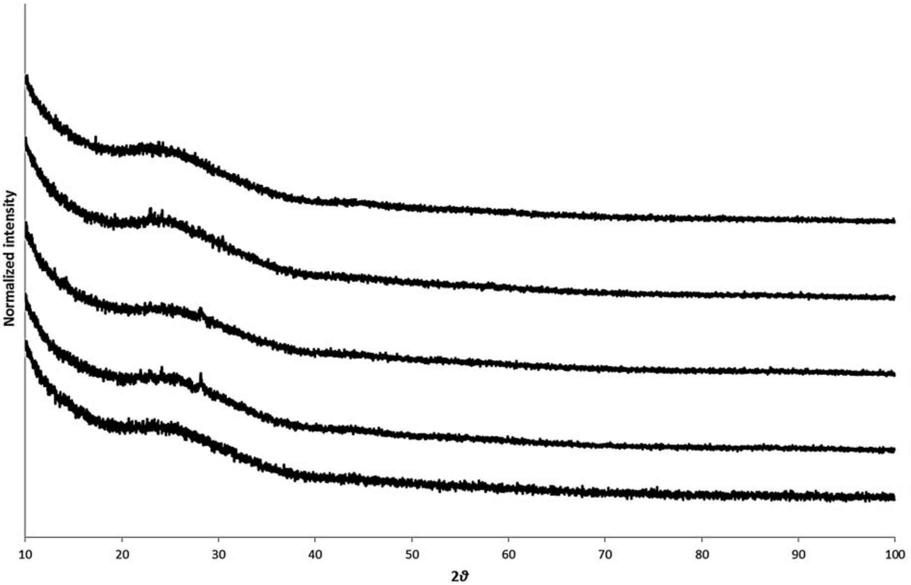

Figure 1.
X-ray diffraction spectra of as-prepared samples of the investigated titanium phosphate glasses.

13.4° and 18.6° respectively. From the software analysis, it was shown that these peaks corresponded to the spectra for $NaCa(PO_3)_3$. Thus, the decrease in intensity of this peak from Ti0 to Ti7 was consistent with the disappearance of $NaCa(PO_3)_3$ as the main phase in the glass. Similarly, the peak corresponding to dotted

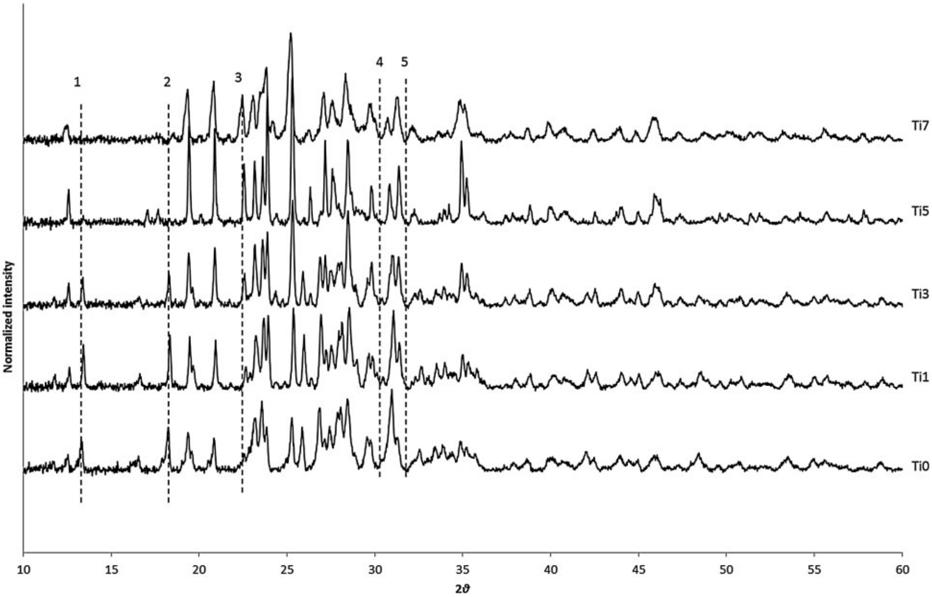

Figure 2.
X-ray diffraction spectra of crystallised samples of the investigated titanium phosphate glasses.

line 3 at approximately 22.5° was found to belong to CaP_2O_6, and the increased intensity of this peak from Ti0 to Ti7 helped to explain the emergence of CaP_2O_6 as the dominant phase in the glass. Further variations in different peaks could be similarly interpreted (e.g. the peaks between dotted lines 4 and 5) but it was difficult to assign these peaks to specific phases.

It is worth noting that the trends in the XRD results obtained for titanium metaphosphate glasses containing 50 mol % P_2O_5 are broadly similar to those obtained for titanium ultraphosphate glasses containing 55 mol% P_2O_5[17] and polyphosphate glasses containing 45 mol% P_2O_5.[18]

High-Temperature X-Ray Diffraction

Figure 3 shows combination plots for Ti0 and Ti1 glasses where the DTA trace, ambient XRD spectrum and contour XRD plot have been included in the same graph (the HT-XRD contours at 29° and 39° and shifting towards lower 2θ values can be attributed to the underlying platinum electrode; fluctuations in these contours are dependent on the thickness of the glass specimen on top of the electrode).

The plots reveal close correlations between three distinct sets of experimental data, namely DTA, XRD and HT-XRD. To illustrate using the Ti0 plot (Figure 3 (a)), the crystallisation peak in the DTA trace occurred at 593°C, which corresponded to a series of events at 2θ values of 20.5°, 23.2°, 25.5°, 27.3°, 27.9°, 29.1°, 29.3° and 34.4°. Analysis of the ambient XRD spectrum obtained for the sample crystallised at a temperature of 600°C revealed that $NaCa(PO_3)_3$ is formed at approximately the same 2θ values. Thus, we could reasonably demonstrate that the crystallisation peak at 593°C corresponds to the formation of $NaCa(PO_3)_3$ as the dominant phase in the glass. Using the same approach for the Ti1 glass (Figure 3(b)), it could be determined that the first and second crystallisation peaks, which significantly overlap with each other, correspond to calcium phosphate [CaP_2O_6; ICDD no.: 11–39] and sodium calcium phosphate [$NaCa(PO_3)_3$; ICDD no.: 23–669]. Similar results were obtained for the Ti3–7 glasses (graphs not shown), although it should be noted that an increase in the TiO_2 content resulted in HT-XRD plots with events occurring at higher temperatures; also, fewer such events were recorded in the HT-XRD spectra and the correspondence between the sets of data was not as strong. HT-XRD data have not been obtained previously for 45 mol% and 55 mol% P_2O_5 glasses; however, a similar analysis was carried out previously for five-component P_2O_5– CaO– Na_2O–TiO_2–SrO glasses[14] and a similar relationship between the DTA, XRD and HT-XRD data was observed. Thus, from an overall perspective, the correlations between these different sets of data points to the strong structure-property relationships that exist in these glasses.

Conclusion

Titanium metaphosphate glasses having compositions of $0.5P_2O_5$–$0.4CaO$–$(0.1–x)$ Na_2O–$xTiO_2$ ($x = 0.00$–0.07 mol fraction) were prepared by the melt-quench method and their structure at the phase level was analysed by means of ambient x-ray diffraction (XRD) and high-temperature XRD (HT-XRD) techniques. Ambient XRD spectra of powdered samples of the as-prepared glass revealed their amorphous nature. Crystallised glass powders were found to contain phases such as [$NaCa(PO_3)_3$; ICDD no.: 23–669], calcium phosphate [CaP_2O_6; ICDD no.: 11–39] and titanium phosphate [TiP_2O_7; ICDD no.: 34–1468] and an increase in TiO_2 content was associated with certain predictable phase transitions in the glass. High-temperature XRD (HT-XRD) contour plots were in good correspondence with the results of both ambient XRD and differential thermal analysis (DTA), thereby demonstrating how three distinct sets of experimental data can be used

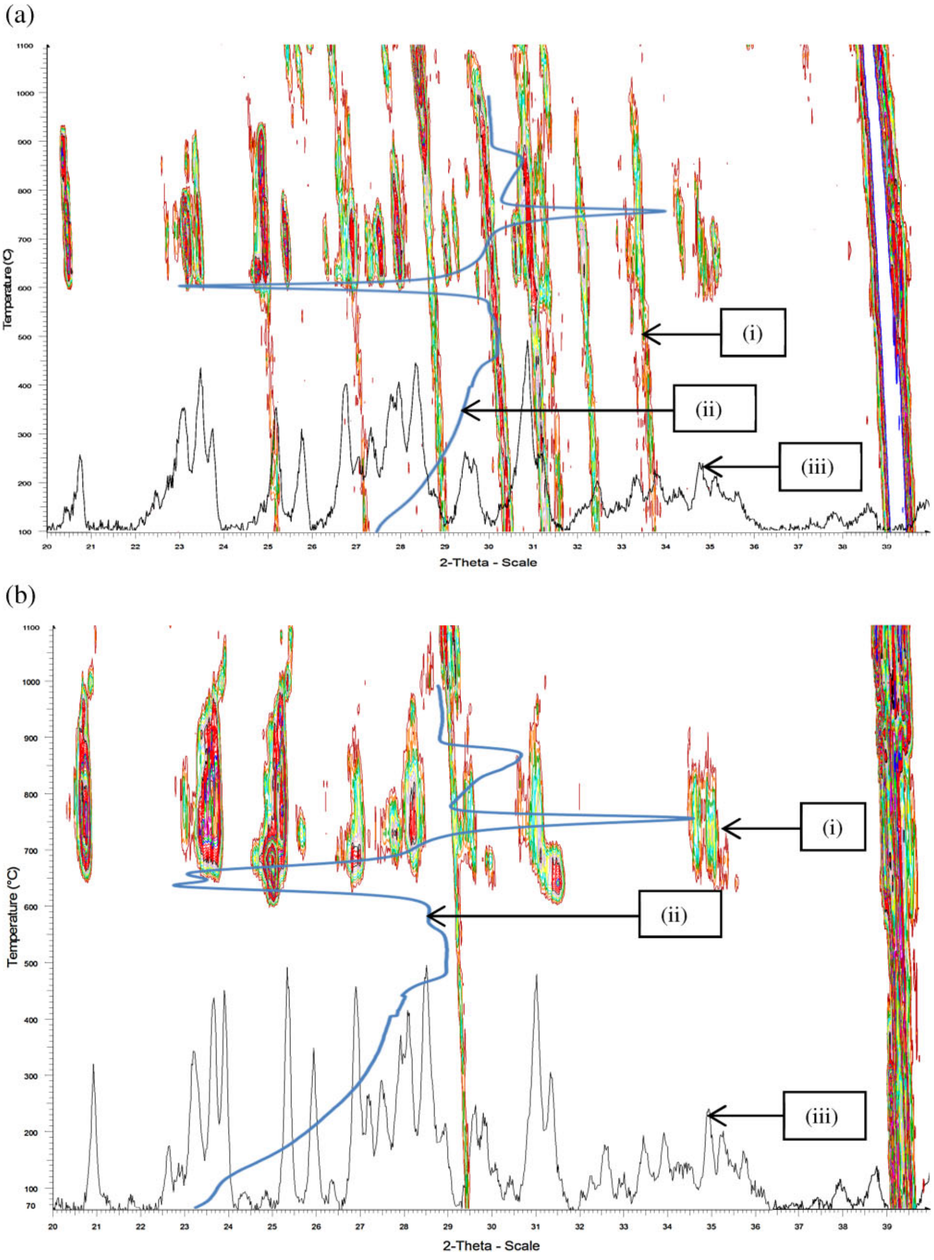

Figure 3.
Combination plot for (a) Ti0 glass and (b) Ti1 glass where (i) contour HT-XRD plot, (ii) DTA trace and (iii) ambient XRD spectrum and are included in the same graph.

together to gain a deeper understanding of the glass structure. Thus, the overall results are of interest from the viewpoint of elucidating the structures of these titanium metaphosphate glasses, which are being used as substrates for hard and soft tissue regeneration with encouraging results.

Acknowledgements: The authors gratefully acknowledge the support provided by the WCU Program through the National Research

Foundation of Korea (NRF) funded by the Ministry of Education, Science and Technology (No. R31–10069). The UCL Graduate School is thanked for the GRS and ORS scholarships provided for NJL.

[1] M. Navarro, M. P. Ginebra, J. Clement, S. Martinez, G. Avila, J. A. Planell, *J Am Ceram Soc.* **2003**, *86*, 1345.

[2] M. Navarro, M. P. Ginebra, J. A. Planell, *Journal of Biomedical Materials Research Part A.* **2003**, *67A*, 1009.

[3] V. Rajendran, A. V. G. Devi, M. Azooz, F. H. El-Batal, *J Non-Cryst Solids.* **2007**, *353*, 77.

[4] A. Kiani, N. J. Lakhkar, V. Salih, M. E. Smith, J. V. Hanna, R. J. Newport, D. M. Pickup, J. C. Knowles, *Philos T R Soc A.* **2012**, *370*, 1352.

[5] J. C. Knowles, *Journal of Materials Chemistry.* **2003**, *13*, 2395.

[6] E. A. Abou Neel W. Chrzanowski, J. C. Knowles, *Acta Biomater.* **2008**, *4*, 523.

[7] E. A. Abou Neel W. Chrzanowski, S. P. Valappil, L. A. O'Dell, D. M. Pickup, M. E. Smith, R. J. Newport, J. C. Knowles, *J Non-Cryst Solids.* **2009**, *355*, 991.

[8] E. A. Abou Neel, J. C. Knowles, *J Mater Sci-Mater M.* **2008**, *19*, 377.

[9] E. A. Abou Neel, T. Mizoguchi, M. Ito, M. Bitar, V. Salih, J. C. Knowles, *Biomaterials* **2007**, *28*, 2967.

[10] A. G. Dias, M. A. Lopes, A. T. T. Cabral, J. D. Santos, M. H. Fernandes, *Journal of Biomedical Materials Research Part A.* **2005**, *74A*, 347.

[11] A. G. Dias, M. A. Lopes, J. D. Santos, A. Afonso, K. Tsuru, A. Osaka, S. Hayakawa, S. Takashima, Y. Kurabayashi, *Journal of biomaterials applications.* **2006**, *20*, 253.

[12] A. S. Monem, H. A. ElBatal, E. M. A. Khalil, M. A. Azooz, Y. M. Hamdy, *J Mater Sci-Mater M.* **2008**, *19*, 1097.

[13] E. A. Abou Neel, L. A. O'Dell, W. Chrzanowski, M. E. Smith, J. C. Knowles, *J Biomed Mater Res B.* **2009**, *89B*, 392.

[14] N. Lakhkar, E. A. Abou Neel, V. Salih, J. C. Knowles, *Journal of biomaterials applications.* **2010**.

[15] N. J. Lakhkar, E. A. Abou Neel, V. Salih, J. C. Knowles, *J. Mater. Sci.-Mater. M.* **2009**, *20*, 1339.

[16] N. J. Lakhkar, J. H. Park, N. J. Mordan, V. Salih, I. B. Wall, H. W. Kim, S. P. King, J. V. Hanna, R. A. Martin, O. Addison, J. F. Mosselmans, J. C. Knowles, *Acta Biomater.* **2012**, *8*, 4181.

[17] A. Kiani, J. V. Hanna, S. P. King, G. J. Rees, M. E. Smith, N. Roohpour, V. Salih, J. C. Knowles, *Acta Biomater.* **2012**, *8*, 333.

[18] A. Kiani, L. S. Cahill, E. A. Abou Neel, J. V. Hanna, M. E. Smith, J. C. Knowles, *Mater. Chem. Phys.* **2010**, *120*, 68.